

## Synthesis, Thermal Characterization and *in vitro* Antibacterial Assessment of Co(II) and Cd(II) Complexes of Schiff Base Derived from Amoxicillin and Thiophene-2-carbaldehyde

N.K. CHAUDHARY\*<sup>ORCID</sup> and B. GURAGAIN

Bio-inorganic and Materials Chemistry Research Laboratory, Mahendra Morang Adarsh Multiple Campus, (Tribhuvan University), Biratnagar, Nepal

\*Corresponding author: E-mail: chem\_narendra@yahoo.com

Received: 18 December 2018;

Accepted: 25 January 2019;

Published online: 27 February 2019;

AJC-19311

A novel  $A_{MX}T_{C2}$  ligand was prepared by simultaneous stirring and refluxing of an equimolar mixture of amoxicillin and thiophene-2-carbaldehyde in methanol and was further used to synthesize metal complexes by metalation with cobalt and cadmium salts, taking ligand metal ratio 2:1. They were characterized by elemental microanalysis, FT-IR, mass, UV-visible,  $^1H$  NMR, thermal analysis, magnetic moment and molar conductance measurements. The coordination sites in the ligand were verified by their comparative and extensive spectral studies. The detailed exploration of the data suggested octahedral geometry for  $Co-A_{MX}T_{C2}$  and tetrahedral geometry for  $Cd-A_{MX}T_{C2}$  complexes. The thermodynamic and kinetic parameters such as  $E^*$ ,  $\Delta H^*$ ,  $\Delta S^*$  and  $\Delta G^*$  of various decomposition steps were calculated from TGA curves using the Coats-Redfern method. The molar conductivity data suggested non-electrolytic nature of the complexes. SEM analysis was done to observe their surface morphology. The geometry optimization of the proposed molecular structure of the complexes was achieved by running MM2 calculation in Gaussian supported Cs-ChemOffice Ultra-11 program software. The biological activities had been evaluated *in vitro* against *E. coli*, *K. pneumonia*, *P. vulgaris* and *S. aureus* pathogens in order to assess their antibacterial potency. The biological data revealed better growth inhibitory action of the ligand and metal complexes with bacterial pathogens.

**Keywords:** Amoxicillin, Thiophene-2-carbaldehyde, Schiff base, Thermal study, Antibacterial activity.

### INTRODUCTION

Although new strategies for the treatment of microbial infections by the use of several metal-based drugs have been practiced and improved. But, the burden of antimicrobial resistance is still a most exciting problem for the human being [1,2]. The current chemistry research explores a wide range of applications of metals in the pharmaceutical industries. Metals bear the ability to form complex with both inorganic and organic compounds and change their biological and physiological profiles. However, the emerging drug resistance is a question of great human concern. Therapeutic failure of most of the drug candidates is the burning issue of current pharmaceutical research and therefore, it requires intensive study to explore new therapeutic drugs with higher efficacy and minimum side effects [3]. Transition metal complexes of Schiff base have paid great attention in the recent years due to their easy accessibility for synthesis, stability and various

biological activities such as antibacterial [4,5], antifungal [6,7], antidiabetic [8], anti-inflammatory [9,10], antitumor and antiviral [11]. Besides their biological role, several other applications such as catalytic, corrosion inhibition effect [12], industrial and electronic applications [13] further enhance their importance. Schiff base is a very popular discovery of past chemical research and the ability for the formation of metal complexes has been increasing the dimension of modern coordination chemistry. The imine group ( $CH=N$ ) of Schiff base is a key structural part which is found in various natural compounds of biological significance. In particular, metals exhibit a prominent role in the redox chemistry of several biomolecules and thereby change their functional behaviour. Cobalt is a metallo-element found in several natural bio-molecules. So studies of its transition metal complexes with Schiff base are of great importance. Moreover, cadmium has toxic effects in the biological system and creates several undesired side effects in the human health [14]. Cadmium toxicity may be ascribed to

the interaction with metallo-proteins or homeostasis with essential metal ions. But as mentioned in the plethora of literature, cadmium based transition metal complexes possess biological significance [15] and eventually, we have selected these two metals for the synthesis of Schiff base metal complexes. Amoxicillin, itself is a broad spectrum  $\beta$ -lactam antibiotic belonging to the class penicillin. Thiophene-2-carbaldehyde is a heteroaromatic aldehyde found in many biological systems [16]. Transition metal complexes of Schiff base with thiophene functionalities will be of special research interest because of their roles in metabolic reactions such as drug interaction with biomolecules.

Reviewing all these facts and in view of our continuing interest in antibiotic research, we designed and synthesized penicillin based novel Schiff base ligand containing  $\beta$ -lactam and thiophene functionalities by the simple condensation reaction of amoxicillin trihydrate and thiophene-2-carbaldehyde. The work was extended by synthesizing its cobalt and cadmium complexes with a special interest in the investigation of their *in vitro* antibacterial efficacy with some Gram-positive and Gram-negative bacteria. The ligand and metal complexes were fully characterized by spectroscopic techniques and thermogravimetric studies. The proposed geometry of the complexes as suggested by spectroscopic techniques was optimized by running MM2 calculations in CsChemoffice 3D ultra software that showed minimum optimization energy.

## EXPERIMENTAL

All the chemicals were of analytical reagent grade (AR) and procured from Duchefa Biochemie Netherland ( $A_{MX}$ ), Spectrochem Mumbai Pvt. Ltd. ( $T_{C2}$ ), Sd. Fines and Qualigens. Amoxicillin trihydrate ( $A_{MX}$ ), thiophene-2-carbaldehyde ( $T_{C2}$ ) and metal salts ( $MCl_2 \cdot xH_2O$ ) ( $M = Co$  and  $Cd$ ,  $x = 6$  and  $0$ ) were used as supplied without further purification. Distilled methanol was used as the solvent for the synthesis. All the glass wares used were cleaned by double distilled water and were perfectly dried.

The elemental microanalysis (C, H, N and S) of the ligand and complexes was investigated by carrying the experiment in Elemental vario EL III model analyzer. pH measurement was done in Elico-16 digital pH meter. Molar conductivity of the complexes was measured in  $10^{-3}$  (M) DMSO solutions using Labtronics auto digital conductivity meter (LT 16 model) with a cell having cell constant of 0.98. The FT-IR spectra were recorded on Perkin Elmer 783 FT-IR spectrophotometer in the wavelength region  $400-4000\text{ cm}^{-1}$  as KBr pellets.  $^1H$  NMR and  $^{13}C$  NMR spectra were recorded on BRUKER Avance (III) 400 MHz spectrometer with operating frequency of 400 MHz using DMSO- $d_6$  solvent referenced to TMS as the internal standard. Mass spectra were recorded on Agilent 6520 Q-TOF mass spectrometer equipped with an electrospray ionization source in positive mode under the mass range of  $m/z$  100 to 1100. Electronic absorption spectra were recorded on single beam microprocessor Labtronics UV-Vis. spectrophotometer (LT-290 model) from 200 to 1000 nm in DMSO solvent. TGA/DTA analyses were carried out in the nitrogen atmosphere in Perkin Elmer thermal analyzer with a linear heating rate of  $10\text{ }^\circ\text{C min}^{-1}$  in the range of 40 to  $750\text{ }^\circ\text{C}$ . SEM micrographs of

the complexes were recorded on JEOL JSM-6390 LV scanning electron microscope. Molecular modeling was accomplished by running energy optimization job through MM2 calculation supported in ChemOffice software program. The biological activity was carried out by the modified Kirby Bauer paper disc diffusion technique.

**Synthesis of ligand ( $A_{MX}T_{C2}$ ):** The  $A_{MX}T_{C2}$  ligand was prepared by adding  $T_{C2}$  (3 mmol, 0.3 mL, 0.3364 g) to homogeneously stirred hot methanolic solution of amoxicillin trihydrate (3 mmol, 1.258 g). The solution of amoxicillin trihydrate was previously made slightly alkaline before addition of  $T_{C2}$  by adding few drops of alcoholic NaOH solution. The mixture was refluxed for several hours to ensure for its formation, which was confirmed by preliminary observation of the colour of the solution. Yellow colouration of the solution (which was initially colourless) indicated the formation of ligand. The solution was concentrated and allowed to cool. The bright yellow solid product was separated by the slow diffusion process, purified by recrystallization from hot methanol and dried over anhydrous calcium chloride.

**Synthesis of metal complexes:**  $Co-A_{MX}T_{C2}$  and  $Cd-A_{MX}T_{C2}$  complexes of  $A_{MX}T_{C2}$  ligand were synthesized as described in the literature [17-19]. To the hot solution of  $A_{MX}T_{C2}$  (1 mmol, 0.473 g), the methanolic solution of  $MCl_2 \cdot xH_2O$  (0.5 mmol,) was added drop-wise with constant stirring. The reaction mixture was set for reflux for 8 h with alternate stirring in order to facilitate the easy approach of the ligand for coordination with metal ions. The coloured solution of  $Co-A_{MX}T_{C2}$  and  $Cd-A_{MX}T_{C2}$  complexes was observed, which on slow cooling at room temperature produced coloured solids. The products were separated, filtered, washed with methanol and dried over anhydrous calcium chloride.

**Antibacterial assessment:** The antibacterial sensitivity of  $A_{MX}T_{C2}$  ligand and its cobalt(II) and cadmium(II) complexes were assessed *in vitro* against clinical pathogenic bacteria such as *E. coli*, *K. pneumonia*, *S. aureus* and *P. vulgaris* by standard Kirby-Bauer paper disc diffusion method and employing Mueller-Hinton's agar media for bacterial growth [20]. The fresh bacterial culture was revived in tryptone soya broth by incubating for 2 h at  $37\text{ }^\circ\text{C}$  for better and complete growth. The broth was swabbed over agar media, prepared in Petri plates. The well-sterilized paper discs of 5 mm diameter (Whatmann no. 1) impregnated with test compounds prepared in DMSO were stuck on the previously seeded bacterial culture [21]. Amikacin  $30\text{ }\mu\text{g/disc}$  of 6 mm size (HIMEDIA co.) was used as a standard reference (+ve control). The antibacterial activity of the test compounds was also compared with amoxicillin trihydrate. They were incubated at  $37\text{ }^\circ\text{C}$  and the diameter of inhibition zone around each disc was measured after 36 h of incubation by using antibiogram zone measuring scale [22].

## RESULTS AND DISCUSSION

**Physical characterization:** Table-1 reports microanalytical (C, H, N & S) data of the synthesized  $A_{MX}T_{C2}$  ligand and its two metal complexes. The experimental found data of the elemental analysis are in good agreement with the calculated values and support  $ML_2$  type geometry of the complexes with 1:2 metal ligand ratio. The complexes were found non-hydro-

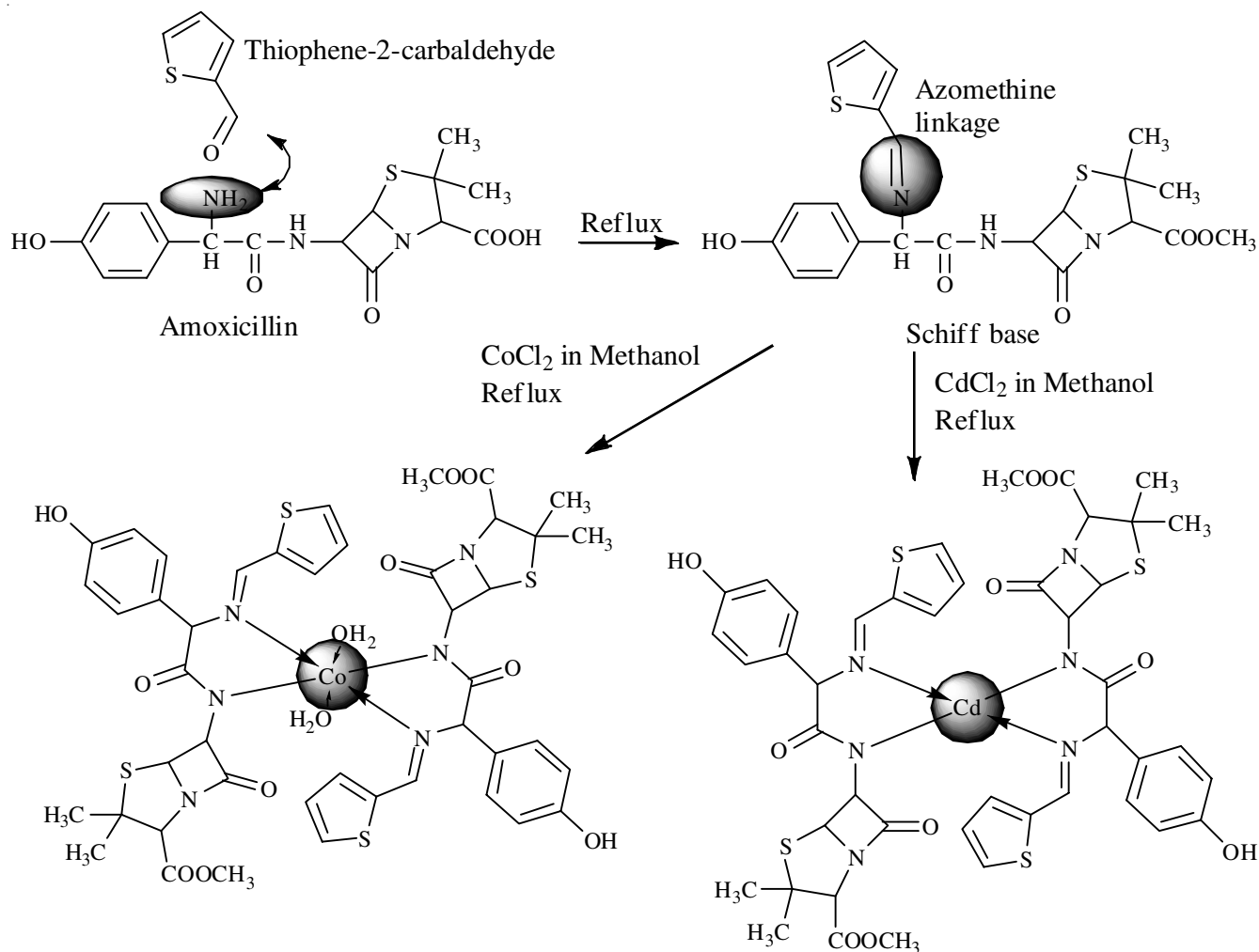


TABLE-1  
PHYSICAL PROPERTIES AND MICRO ANALYTICAL DATA OF LIGAND ( $A_{MX}T_{C2}$ ) AND METAL COMPLEXES

Complex	m.f.	m.w.	Colour	Calculated (Found) (%)				
				C	H	N	O	S
$L = A_{MX}T_{C2}$	$C_{22}H_{23}N_3O_5S_2$	473	Bright yellow	55.80 (55.33)	4.90 (4.87)	8.87 (8.80)	16.89 (16.80)	13.54 (13.16)
$Co-A_{MX}T_{C2} \cdot 2H_2O$	$C_{44}H_{48}N_6O_{12}S_4Co$	1039	Dark green	50.81 (50.82)	4.65 (4.80)	8.08 (7.89)	18.46 (18.42)	12.33 (12.35)
$Cd-A_{MX}T_{C2}$	$C_{44}H_{44}N_6O_{10}S_4Cd$	1058	Orange	49.97 (49.80)	4.19 (4.24)	7.95 (7.80)	15.13 (15.10)	12.13 (12.40)

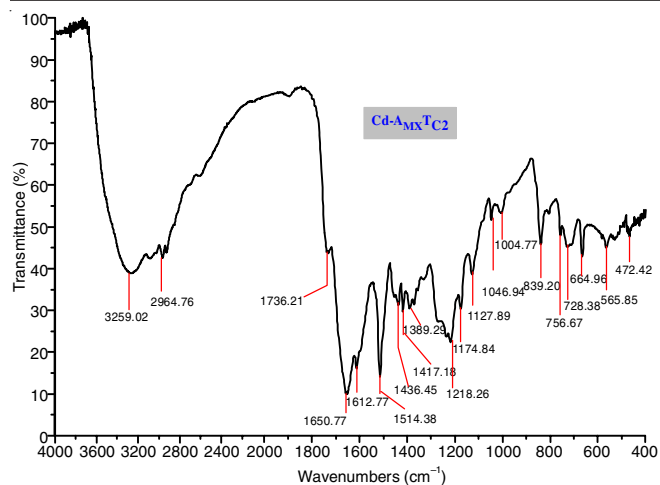
scopic, air stable, insoluble in water but soluble in mild polar organic solvents like DMSO and DMF. The molar conductivity study revealed non-electrolytic nature of the compounds.

**FT-IR spectroscopy:** The solution for the preliminary structural aspects of ligand and its metal complexes can be interpreted on the basis of their FT-IR spectral comparison which provides valuable information about the coordination sites that may be involved in the chelation process. The details of the absorption frequencies of the  $A_{MX}T_{C2}$  ligand and its metal complexes are presented in Table-2 and the FT-IR spectra

of  $Cd-A_{MX}T_{C2}$  is shown in Fig. 1. The binding mode of the metal ions can be assured from the difference in IR band positions of  $A_{MX}T_{C2}$  ligand and metal complexes. The strong intensity band observed at  $1655.29\text{ cm}^{-1}$ , characteristic to azomethine ( $C=N$ ) stretch for  $A_{MX}T_{C2}$  has shifted to  $1650.67$  and  $1650.77\text{ cm}^{-1}$  for  $Co-A_{MX}T_{C2}$  and  $Cd-A_{MX}T_{C2}$  complexes respectively and supported the coordination of azomethine nitrogen to the metal center [23]. This fact has further supported by the appearance of new bands at  $462.77\text{ cm}^{-1}$  for  $Co-A_{MX}T_{C2}$  and at  $467.42$

TABLE-2  
FTIR SPECTRAL DATA OF LIGAND ( $A_{MX}T_{C2}$ ) AND ITS METAL COMPLEXES

Compounds	$\nu(NH/OH)$	$\nu(C=O)$ carboxylic	$\nu(C=N)$	$\nu(C=O)$ lactam	$\nu(CH_3)$	$\nu(COO)$	$\nu(M-N)$
$L = A_{MX}T_{C2}$	3296.31 (br)	1734.61	1655.29 (s)	1612.99	2963.65	1515.01	–
$Co-A_{MX}T_{C2} \cdot 2H_2O$	3355.52 (br)	1742.19	1650.67 (s)	1612.45	2966.17	1513.73	462.77
$Cd-A_{MX}T_{C2}$	3259.02 (br)	1736.21	1650.77 (s)	1612.77	2964.76	1514.38	467.42

Fig. 1. IR spectrum of Cd-A<sub>MX</sub>T<sub>C2</sub> complex

cm<sup>-1</sup> for Cd-A<sub>MX</sub>T<sub>C2</sub> complexes, which are assignable for metal-nitrogen coordination. Non-involvement of carboxylate group in the coordination process has been assigned by almost no shift in band positions observed for the stretching vibrations of carboxylate (COO<sup>-</sup>) group. The absorption bands in the range of 2966-2917 cm<sup>-1</sup> in all the synthesized compounds could be assigned to the methyl C-H stretch [24]. A weak but sharp band observed at 1612.99 cm<sup>-1</sup> assignable for ν(C=O) lactam is restored in the metal complexes [25]. Moreover, change in IR absorption bands from 3355.52 to 3296.31 cm<sup>-1</sup> for N-H stretch of A<sub>MX</sub>T<sub>C2</sub> and metal complexes provides good conformity for the coordination of metal ions with the deprotonated nitrogen of (NH) group of substituted amide [26].

**<sup>1</sup>H NMR spectral analysis:** The <sup>1</sup>H NMR spectra of A<sub>MX</sub>T<sub>C2</sub> ligand and Cd-A<sub>MX</sub>T<sub>C2</sub> complex have been recorded in DMSO-*d*<sub>6</sub> solvent and their comparison provides valuable information about the proton environment and possible coordination sites of the ligand. The spectra are virtually indistinguishable with minor shifting of the peaks and their intensity. The azomethine proton appeared as a multiplet at 9.704 and 9.95 ppm for A<sub>MX</sub>T<sub>C2</sub> and Cd-A<sub>MX</sub>T<sub>C2</sub> respectively [27]. The methyl protons signal was observed in the range of 0.8 to 1.14 and 0.9 to 1.4 ppm for A<sub>MX</sub>T<sub>C2</sub> ligand and Cd-A<sub>MX</sub>T<sub>C2</sub> complex, respectively. The four aromatic protons of the amoxicillin moiety have confirmed by the appearance of resonance signal in the range between 6.4 and 7.12 ppm. The heterocyclic ring protons of the ligand moiety in both A<sub>MX</sub>T<sub>C2</sub> and Cd-A<sub>MX</sub>T<sub>C2</sub> showed resonance signal in the range of 7.7 to 7.9 ppm. The amide NH proton of the ligand resonated at 8.04 ppm and the absence of this signal in complex may suggest metal coordination to amide N atom.

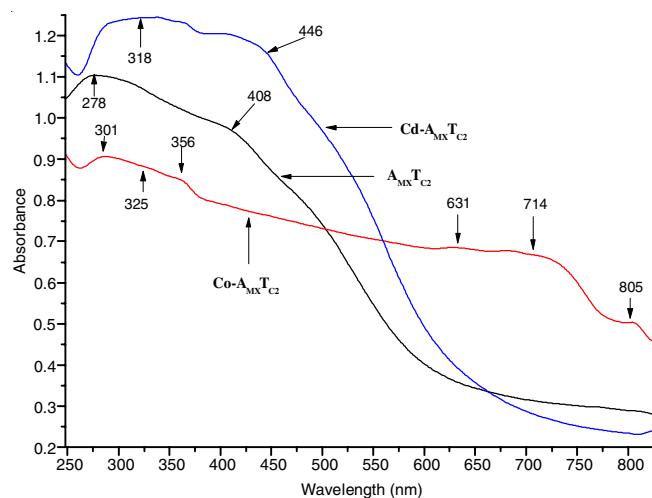
**Mass spectral analysis:** The ESI mass spectrum of A<sub>MX</sub>T<sub>C2</sub> showed a molecular ion peak at *m/z* 473.57 amu corresponding to molecular ion peak [M<sup>+</sup>] and it might confirm the proposed molecular formula of A<sub>MX</sub>T<sub>C2</sub>. Similar ESI-MS spectrum of the Co-A<sub>MX</sub>T<sub>C2</sub> showed molecular ion peak at *m/z* 1039 amu. The corresponding molecular ion peak for Cd-A<sub>MX</sub>T<sub>C2</sub> complex was observed at 1058 amu.

**Electronic absorption and conductivity measurement:** The electronic absorption spectra of A<sub>MX</sub>T<sub>C2</sub> and its metal complexes were recorded in DMSO solution in the wavelength range of 250 to 850 nm and the spectral data are presented

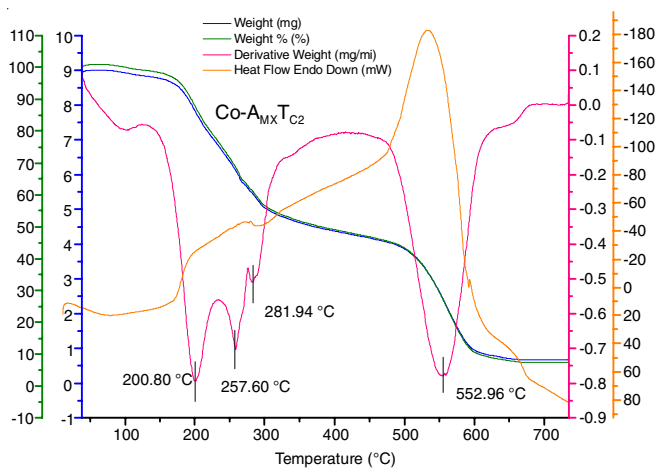
in Table-3. Fig. 2 presents UV/visible spectra of ligand and its metal complexes. The absorption bands at lower wavelength region for A<sub>MX</sub>T<sub>C2</sub> ligand and its metal complexes may be attributed to π→π\* and n→π\* transitions of thiophene ring, the aromatic ring and azomethine moiety of A<sub>MX</sub>T<sub>C2</sub> [28]. A<sub>MX</sub>T<sub>C2</sub> exhibited absorption band at 408 nm corresponding to intra-ligand charge transfer (ILCT) transition. However, in the metal complexes, the positions of absorption bands in the UV region have been shifted to higher wavelengths specifying ligand-metal coordination. Besides of the high energy transition bands, some additional and characteristic bands in the visible region were seen for Co-A<sub>MX</sub>T<sub>C2</sub> complex, which was due to *d-d* transition. The Co-A<sub>MX</sub>T<sub>C2</sub> exhibits three absorption bands in the visible region at 631, 714 and 805 nm, which were assigned to <sup>4</sup>T<sub>1g</sub>(F)→<sup>4</sup>T<sub>1g</sub>(P), <sup>4</sup>T<sub>1g</sub>(F)→<sup>4</sup>A<sub>2g</sub> and <sup>4</sup>T<sub>1g</sub>(F)→<sup>4</sup>T<sub>2g</sub> transitions respectively, specifying hexa-coordination octahedral geometry [29,30]. This geometry of Co-A<sub>MX</sub>T<sub>C2</sub> complex has further supported by its magnetic moment value 5.1 BM. The Cd-A<sub>MX</sub>T<sub>C2</sub> has completely filled *d*<sup>10</sup> electronic configuration and no *d-d* transition bands are expected for this, rather ligand to metal charge transfer band can be assigned for the absorption observed in the visible region of the spectrum [27]. Tetrahedral geometry has been assigned for this complex which was supported by its diamagnetic nature with magnetic moment value, 0 BM. The measured conductivity values for the ligand and complexes deliver their nonelectrolytic nature.

TABLE-3  
UV/VISIBLE AND CONDUCTIVITY DATA OF  
LIGAND (A<sub>MX</sub>T<sub>C2</sub>) AND ITS METAL COMPLEXES

Comp.	Peak positions (nm)	Assignment	Conductance (μ siemen/cm)
L = A <sub>MX</sub> T <sub>C2</sub>	278	π→π*	5.75
	408	n→π* (ILCT)	
Co-A <sub>MX</sub> T <sub>C2</sub>	301	π→π*	25.2
	325	π→π*	
	356	n→π*	
	631	<sup>4</sup> T <sub>1g</sub> (F)→ <sup>4</sup> T <sub>1g</sub> (P)	
	714	<sup>4</sup> T <sub>1g</sub> (F)→ <sup>4</sup> A <sub>2g</sub>	
Cd-A <sub>MX</sub> T <sub>C2</sub>	805	<sup>4</sup> T <sub>1g</sub> (F)→ <sup>4</sup> T <sub>2g</sub>	11.12
	318	n→π*	
	446	LMCT	

Fig. 2. UV/visible spectrum of A<sub>MX</sub>T<sub>C2</sub> ligand and its metal complexes

**Thermal study:** Thermogravimetric analysis is a tool to evaluate the thermal stability of the complexes in terms of mass loss with respect to the variation of temperature. Fig. 3 presents thermogram of Co-A<sub>MX</sub>T<sub>C2</sub> complex that have been carried out at a linear heating rate of 10 °C/min with a sample size of 8.914 mg. Table-4 reports thermal decomposition parameters of metal complexes. The Co-A<sub>MX</sub>T<sub>C2</sub> shows non-isothermal decomposition in three distinct steps in between temperature range of 153 to 602 °C and after this, thermogram gives horizontal plateau, indicating the occurrence of stable cobalt oxide residue. A small mass loss is observed in the temperature range of 70 to 130 °C with DTG temperature 96 °C and DTA temperature 103.84 °C with endothermic effect and this could be assigned the loss of moisture or non-coordinated H<sub>2</sub>O molecules [28]. The first decomposition step involving TG plateau in between the temperature range of 153.95 °C and 227.27 °C with DTG temperature 200.8 °C is assigned to the loss of two coordinated H<sub>2</sub>O molecules. The corresponding mass loss for the first step is 12.263 %. The second step involves a mass loss of 30.94 % of the total sample size and this may attribute the loss of ligand moiety. The third decomposition step involves the complete loss of organic ligand moiety with mass loss of 71.833 % of the total sample size and finally, the thermogram became horizontal, which possibly indicates the formation of stable cobalt oxide residue. The corresponding DTG temperatures for second and third steps are 257.60 °C and 552.96 °C. The sample size for Cd-A<sub>MX</sub>T<sub>C2</sub> complex was 5.795 mg. The Cd-A<sub>MX</sub>T<sub>C2</sub> complex shows non-isothermal decomposition in four distinct steps in between the temperature range of 72.06 °C and 314.23 °C. The first decomposition step involves mass loss of 3.085 % with corresponding DTG temperature 90.11 °C

Fig. 3. Thermogram of Co-A<sub>MX</sub>T<sub>C2</sub> complex

and this may attribute the loss of lattice water and moisture. In the other three consecutive decomposition steps, there is very small temperature range variation and these could give the impression of a single step with shoulder peaks of one another. The corresponding mass loss in these steps attributes the evaporation of organic ligand moiety.

**Kinetic parameters:** The kinetic and thermodynamic energy parameters associated with various decomposition steps in the thermal process are very important for the evaluation of the nature of complexes and also a quick technique for assigning the stability of the material substances. The present investigation used a popular Coats-Redfern equation to extract these parameters from DTG and DTA curves of the metal complexes. The Coats-Redfern equation is given as:

$$\ln\left(-\frac{\ln(1-\alpha)}{T^2}\right) = \ln\left(\frac{AR}{\beta E^*}\right) - \frac{E^*}{RT}$$

here  $\alpha$  represents fraction decomposed at T K,  $E^*$  = activation energy, R = gas constant, A = pre-exponential factor and  $\beta$  is the linear heating rate (10 °C min<sup>-1</sup>). The equation was solved for a straight line ( $y = mx + c$ ) whose correlation factor (r) value gave a best linear plot. The energy of activation was evaluated from its slope and its intercept gave the value of A [31-33]. The other thermodynamic parameters ( $\Delta H^*$ ,  $\Delta S^*$ ,  $\Delta G^*$ ) were evaluated by using standard equations:

$$\Delta S^* = R \ln\left(\frac{Ah}{k_B T}\right)$$

$$\Delta H^* = E^* - RT$$

$$\Delta G^* = \Delta H - T\Delta S^*$$

In the equation,  $k_B$  represents Boltzmann constant and h represents Planck's constant. The calculated values of thermodynamic and kinetic parameters of the investigated complexes are listed in Table-5. Following remarks have been carried out in regards to the complexes.

(a) The first step in both the complexes involves loss of H<sub>2</sub>O molecules, also called dehydration step. The negative values of  $\Delta S^*$  in this step indicates more ordered activated state of the complex and the decomposition is slower than the normal. The second step for Co-A<sub>MX</sub>T<sub>C2</sub> complex involves loss of ligand part with  $+\Delta S^*$  value and this may support spontaneous degradation. Moreover, third step corresponds complete loss of organic ligand moiety and also has  $-\Delta S^*$  value. The decomposition steps in the Cd-A<sub>MX</sub>T<sub>C2</sub> complex show  $+\Delta S^*$  values and this reflects spontaneous decomposition process.

(b) The activation energy  $E^*$  values in both the complexes are in increasing order with the increase in temperature and

TABLE-4  
THERMAL DECOMPOSITION DATA OF METAL COMPLEXES

Complex	Steps	$\Delta_m$ % found	TG plateau (°C)	T <sub>DTG</sub> (°C)	Mass loss	T <sub>DTA</sub> (°C)	Assignment
Co-A <sub>MX</sub> T <sub>C2</sub>	1	12.263	153.95-227.27	200.80	1.740	–	Loss of H <sub>2</sub> O
	2	30.94	242.27-273.38	257.60	0.926	291.22	Loss of ligand
	3	71.833	495.48-601.52	552.96	2.977	541.68	Complete loss of organic ligand
Cd-A <sub>MX</sub> T <sub>C2</sub>	1	3.085	72.06-122.6	90.11	0.437	97.84	Loss of moisture
	2	25.737	198.31-225.21	215.24	0.828	–	Loss of ligand part
	3	39.877	235.58-246.66	238.34	0.395	–	Loss of ligand part
	4	66.228	306.7-314.23	307.62	0.168	–	Complete loss of organic ligand

TABLE-5  
 KINETIC AND THERMODYNAMIC PARAMETERS OF METAL COMPLEXES

Complex	Steps	r	A (S <sup>-1</sup> )	T <sub>max</sub> (K)	E* (kJ)	ΔS* (J)	ΔH* (kJ)	ΔG* (kJ)
Co-A <sub>MX</sub> T <sub>C2</sub>	1	-0.99418	2.63x10 <sup>9</sup>	473.95	118.56	-68.42	114.62	147.05
	2	-0.99271	3.66x10 <sup>21</sup>	530.75	253.98	163.10	249.568	163
	3	-0.99221	2.78x10 <sup>11</sup>	826.11	242.69	-34.28	228.96	94.22
Cd-A <sub>MX</sub> T <sub>C2</sub>	1	-0.99161	1.17x10 <sup>6</sup>	363.26	69.10	-131.18	66.084	113.425
	2	-0.99153	2.30x10 <sup>25</sup>	488.39	267.28	235.72	263.221	148.097
	3	-0.99823	1.09x10 <sup>52</sup>	511.49	541.62	746.03	537.367	155.79
	4	-0.9934	8.57x10 <sup>68</sup>	580.77	801.133	1068.44	796.304	176.04

this confirms their greater stability. The calculated E\* value of Cd-A<sub>MX</sub>T<sub>C2</sub> complex is relatively greater than Co-A<sub>MX</sub>T<sub>C2</sub> complex which is perfectly in good agreement with the electronegative character of the metal ions and also suggests the greater stability of Cd-A<sub>MX</sub>T<sub>C2</sub> complex. The comparative ionic radius of these two metal ions further supports this trend of stability. Being large size of the ligand, hexacoordinated complex is sterically more hindered than tetra-coordinated Cd-A<sub>MX</sub>T<sub>C2</sub> complex. The delocalization of electrons in the chelate ring increases as the ionic radius of metal ions increase and this further provides evidence for the greater stability of the Cd-A<sub>MX</sub>T<sub>C2</sub> complex.

(c) There are no clear trends in the values of enthalpy of activation (ΔH\*) and free energy of activation (ΔG\*). For Co-A<sub>MX</sub>T<sub>C2</sub> complex, the values of ΔH\* and ΔG\* increase from the first step to the second step and then decreased to the third step. This indicates a slower rate of decomposition of the second step than the first and third steps and this may be due to partial loss of ligand in the second step. However in the Cd-A<sub>MX</sub>T<sub>C2</sub> complex, it seems an increasing trend of these values and this indicates the decreasing rate of decomposition in the subsequent steps.

**SEM study:** The antibacterial effect of the metal complexes may change their morphological profiles due to membrane integrity with bacterial cells. Thus SEM study can link the interaction of chemicals with bacterial inhibition [34]. In the present investigation, we just compared the surface morphology of A<sub>MX</sub>T<sub>C2</sub> ligand and its metal complexes which provide fruitful information about the pattern of molecular aggregation in bulk. SEM analytical study provides information about the comparative surface morphology of the ligand and metal complexes. The SEM micrographs of A<sub>MX</sub>T<sub>C2</sub> and metal complexes are given in Fig. 4. The different characteristic shapes and sizes of the particles of Schiff base and metal complexes give

evidence of the metal complexation. SEM micrographs of A<sub>MX</sub>T<sub>C2</sub> and Cd-A<sub>MX</sub>T<sub>C2</sub> resemble broken rock like structure with the glassy appearance with different particle size dimensions. Moreover, the SEM micrograph of Co-A<sub>MX</sub>T<sub>C2</sub> has shown unevenly distributed broken ice-like structure.

**Molecular modeling study:** The experimental aspects for the structural characterization of the synthesized organic ligand and metal complexes can be visualized by theoretical studies based on quantum mechanical calculations in the special designed molecular modeling software [35]. In present study, 3D molecular modeling structure of the proposed ligand and metal complexes was evaluated by CsChemOffice 3D Ultra-11 and ArgusLab (4.0.1) program package, which revealed octahedral geometry for the Co-A<sub>MX</sub>T<sub>C2</sub> and tetrahedral geometry for Cd-A<sub>MX</sub>T<sub>C2</sub> complex. The reasonable and low energy molecular geometries were obtained through manipulation and modification of the molecular coordinates. The energy optimization was repeated several times to find the minimum energy molecular geometry [36-38]. The bonding parameters such as bond length and bond angles data of A<sub>MX</sub>T<sub>C2</sub> and its metal complexes, optimized by MM2 calculation are reported in Table-6 and their 3D molecular structures are presented in Figs. 5 and 6. The molecular mechanical approach uses the Born-Oppenheimer approximation to determine nuclear energy by installing fixed electron distribution in the molecule. The optimized energy of a molecule involves sum of the steric and non-bonded interaction energies [39].

$$E_T = E_{Str} + E_{bend} + E_{tor} + E_{vdw} + E_{oop} + E_{ele}$$

The subscripts in the equation str, bend, tor, vdw, oop and ele represent, respectively stretching, bending, torsional, van der Waals, out of plane and electronic interaction related actions that contribute in the total energy of the molecular system. The molecular mechanics runs a series of iterations to vary

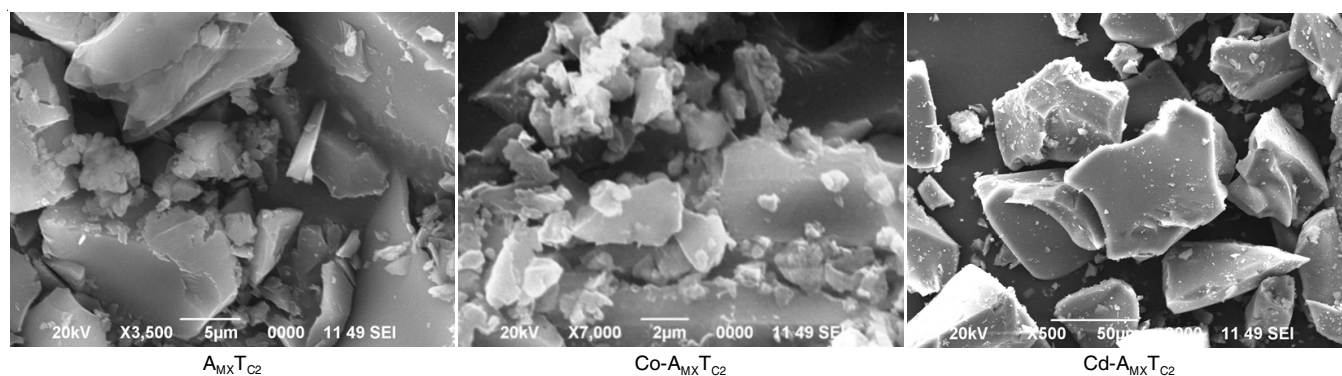
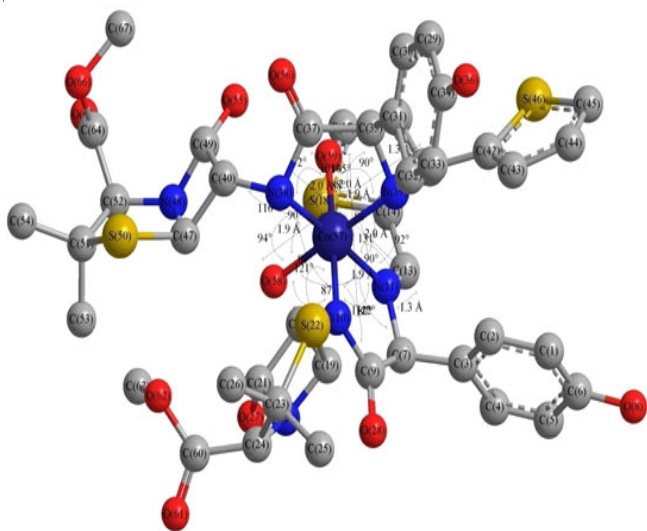
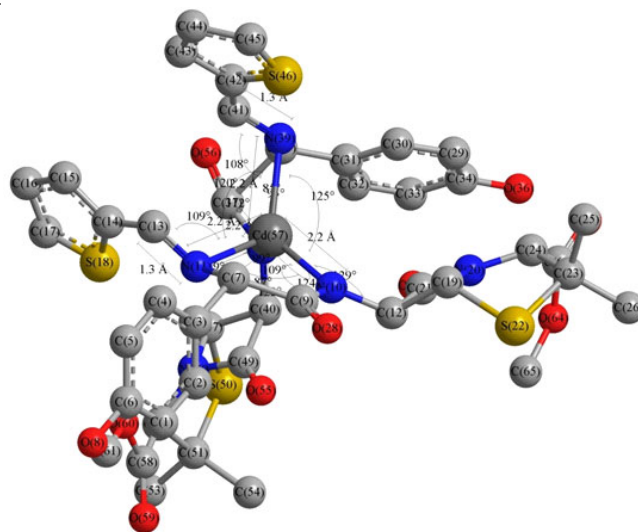

 Fig. 4. SEM images of (a) A<sub>MX</sub>T<sub>C2</sub> (b) Co-A<sub>MX</sub>T<sub>C2</sub> (c) Cd-A<sub>MX</sub>T<sub>C2</sub>

TABLE-6  
SELECTED BOND LENGTHS AND BOND ENERGY PARAMETERS OF LIGAND ( $A_{MX}T_{C2}$ ) AND ITS METAL COMPLEXES

Compounds	Atoms	Bond angles (°)	Atoms	Bond length (Å) (actual/optimized)	Final geom. energy (Kcal/mol)
$L = A_{MX}T_{C2}$			C(28)-N(10)	1.2940 (1.26)	170.5742 (0.2718 au)
			C(8)-C(9)	1.5130 (1.509)	
			C(9)-N(11)	1.3552 (1.369)	
			N(10)-C(8)	1.4548 (1.47)	
Co- $A_{MX}T_{C2}$	O(59)-Co(57)-O(58)	90.4882	N(39)-Co(57)	2.0034	415.635 (0.6623 au)
	O(59)-Co(57)-N(39)	89.9974	N(11)-Co(57)	2.0055	
	O(59)-Co(57)-N(38)	91.5867	N(38)-Co(57)	2.0224	
	O(59)-Co(57)-N(11)	93.1831	N(10)-Co(57)	1.9493	
	O(59)-Co(57)-N(10)	179.6724	O(59)-Co(57)	1.9403 (0.6)	
	O(58)-Co(57)-N(39)	178.6589	O(58)-Co(57)	1.9398 (0.6)	
	O(58)-Co(57)-N(38)	93.6946	N(11)-C(13)	1.31 (1.26)	
	O(58)-Co(57)-N(11)	86.7744	N(39)-C(41)	1.3142 (1.26)	
	O(58)-Co(57)-N(10)	89.3557			
	N(39)-Co(57)-N(38)	87.5415			
	N(39)-Co(57)-N(11)	91.9505			
	N(39)-Co(57)-N(10)	90.1524			
	N(38)-Co(57)-N(11)	175.2034			
	N(38)-Co(57)-N(10)	88.7108			
	N(11)-Co(57)-N(10)	86.5206			
	Co(57)-N(39)-C(41)	106.9165			
	Co(57)-N(39)-C(35)	105.2246			
	Co(57)-N(38)-C(40)	115.7155			
	Co(57)-N(38)-C(37)	101.1432			
Co(57)-N(11)-C(13)	130.8464				
Co(57)-N(11)-C(7)	112.4040				
Co(57)-N(10)-C(12)	121.0231				
Co(57)-N(10)-C(9)	111.5657				
Cd- $A_{MX}T_{C2}$	N(39)-Cd(57)-N(38)	85.3883	N(39)-Cd(57)	2.1604	387.1337 (0.6169 au)
	N(39)-Cd(57)-N(11)	120.1602	N(11)-Cd(57)	2.1650	
	N(39)-Cd(57)-N(10)	125.0552	N(38)-Cd(57)	2.1568	
	N(38)-Cd(57)-N(11)	119.4508	N(10)-Cd(57)	2.1543	
	N(38)-Cd(57)-N(10)	124.2770	N(39)-C(41)	1.2710 (1.26)	
	N(11)-Cd(57)-N(10)	86.7371	N(11)-C(13)	1.2707 (1.26)	
	Cd(57)-N(39)-C(41)	107.8464			
	Cd(57)-N(39)-C(35)	94.8691			
	Cd(57)-N(38)-C(40)	122.0706			
	Cd(57)-N(38)-C(37)	111.9364			
	Cd(57)-N(11)-C(13)	108.6248			
	Cd(57)-N(11)-C(7)	99.1013			
	Cd(57)-N(10)-C(12)	129.2159			
Cd(57)-N(10)-C(9)	109.1985				

Fig. 5. Optimized molecular modeling of Co- $A_{MX}T_{C2}$  complexFig. 6. Optimized molecular modeling of Cd- $A_{MX}T_{C2}$  complex

the structure of the molecules in small amounts in all directions and average the energy to get a minimum and provide a real conformational structure. The observed bond length of azomethine (C=N) bond for  $A_{MX}T_{C2}$  (1.2940 Å) has undergone shift after complexation and supports coordination of azomethine N-atom with the metal ion in the chelation process. The bond angles around Co(II) in the complex are quite near to the octahedral geometry and predicts  $sp^3d^2$  hybridization. The tetrahedral geometry of Cd- $A_{MX}T_{C2}$  is well evidenced by its bond angles data close to  $sp^3$  hybridization. Hence, hexacoordination and tetracoordination of Co- $A_{MX}T_{C2}$  and Cd- $A_{MX}T_{C2}$  as suggested by spectral and analytical data are in a good fit with the molecular modeling data. Hamiltonian UFF operation search in ArgusLab program [40] evaluated final geometrical energy of 170.5742 Kcal/mol for  $A_{MX}T_{C2}$ , 415.635 Kcal/mol for Co- $A_{MX}T_{C2}$  complex and 387.1337 Kcal/mol for the Cd- $A_{MX}T_{C2}$  complex. Optimized energy data revealed Cd- $A_{MX}T_{C2}$  complex more stable than Co- $A_{MX}T_{C2}$  complex. Less stability of Co- $A_{MX}T_{C2}$  complex may be due to steric factor and macromolecular structure of the molecule.

**Antibacterial sensitivity:** The *in vitro* antibacterial sensitivity of  $A_{MX}T_{C2}$  and its two metal complexes were screened to analyze the antibacterial potency against three Gram-negative (*E. coli*, *K. pneumonia* and *P. vulgaris*) and one Gram-positive (*S. aureus*) human pathogenic bacteria. Paper disc diffusion technique was applied to carry out this study. The sensitivity was assessed by measuring the growth inhibition zone around the loaded disc. The antibacterial potency of drug substances was compared and evaluated at their two different concentrations (100 and 50 mcg/ml). The comparative data for the growth inhibition zone is presented in Table-7. The results revealed the excellent antibacterial activity of metal complexes compared to  $A_{MX}T_{C2}$  against Gram-negative bacteria. Moreover,  $A_{MX}T_{C2}$  exhibited better antibacterial activity compared to the metal complexes against Gram-positive bacteria. Cd- $A_{MX}T_{C2}$  has shown better antibacterial potency compared to the Co- $A_{MX}T_{C2}$ . The parent drug amoxicillin was found resistant against Gram-negative bacteria and was found sensitive against *S. aureus*. Amikacin (30 mcg/ml) was used as a standard reference to compare the activity of  $A_{MX}T_{C2}$  and metal complexes against the same microbes under identical experimental conditions. DMSO was used as the solvent for the preparation of solution which showed no activity against microbes. The details of the antibacterial comparison are presented in the bar graph Figs. 7 and 8. The better antibacterial sensitivity of metal complexes may be due to their increased lipophilicity caused by chelation of ligand with metal ions. Chelation makes the complex more stable due to the reduced electronic charge.

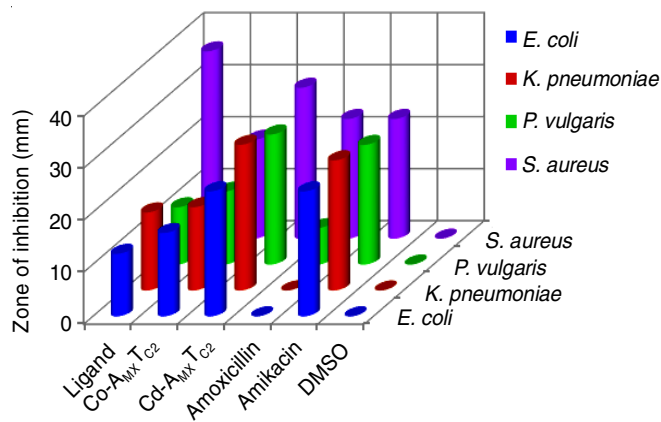


Fig. 7. Bar graph of antibacterial sensitivity at 100 mcg/ml concentration

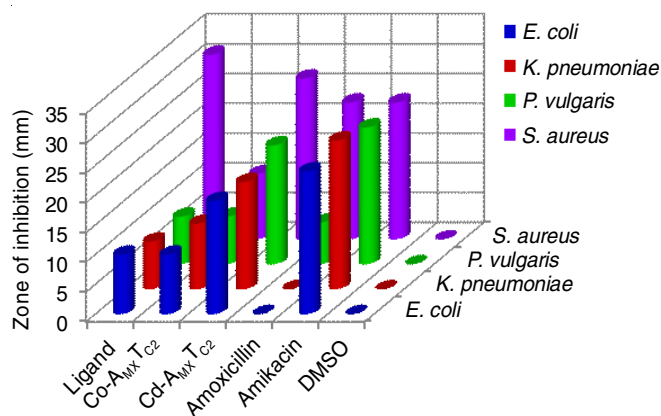


Fig. 8. Bar graph of antibacterial sensitivity at 50 mcg/ml concentration

## Conclusion

The present paper aimed to describe the synthesis of  $A_{MX}T_{C2}$  ligand and its two metal complexes (Co- $A_{MX}T_{C2}$  and Cd- $A_{MX}T_{C2}$ ) with Co(II) and Cd(II) salts. The synthesized compounds were characterized by elemental microanalysis and spectral studies. The elemental analysis revealed  $ML_2$  (M = metal, L =  $A_{MX}T_{C2}$ ) type complexes with 1:2 stoichiometry. Based on spectral studies, the ligand has bonded to a metal center through azomethine N and amide N atoms and assigned octahedral geometry for Co- $A_{MX}T_{C2}$  and tetrahedral geometry for Cd- $A_{MX}T_{C2}$  complexes. Further evidence for their suggested geometry was prevailed by magnetic moment and electronic absorption spectral data. The thermal study revealed the presence of two coordinated  $H_2O$  molecules in Co- $A_{MX}T_{C2}$  complex. The biological potency of the ligand and its metal complexes was assured by their antibacterial evaluation. Such study revealed

TABLE-7  
ANTIBACTERIAL GROWTH INHIBITION DATA OF LIGAND ( $A_{MX}T_{C2}$ ) AND METAL COMPLEXES

Compounds	Diameter of the zone of Inhibition in mm							
	<i>E. coli</i>		<i>K. pneumonia</i>		<i>P. vulgaris</i>		<i>S. aureus</i>	
Concentration (mcg/ml)	100	50	100	50	100	50	100	50
L = $A_{MX}T_{C2}$	12	10	15	8	11	8	36	31
Co- $A_{MX}T_{C2}$	16	10	16	11	14	8	19	11
Cd- $A_{MX}T_{C2}$	24	19	28	18	25	20	29	27
Amox.	0		0		7		23	
Amk. (30 mcg/disc)	24		25		23		23	
DMSO	0		0		0		0	

significant antibacterial activity against all the referenced clinical pathogens. The  $A_{MX}T_{C2}$  ligand exhibited better growth inhibiting activity compared to the parent drug amoxicillin.

### ACKNOWLEDGEMENTS

The authors thank University Grants Commission, Nepal (Award no. SRDIG-73/74-S&T-10) for financial support. The authors declare thanks to Prof. P. Mishra for his invaluable discussion and also acknowledge to Department of Chemistry, Mahendra Morang Adarsh Multiple Campus, Biratnagar for providing research facility, SAIF, STIC Cochin and SAIF, IIT Bombay for analytical and spectral results.

### CONFLICT OF INTEREST

The authors declare that there is no conflict of interests regarding the publication of this article.

### REFERENCES

- S.B. Zaman, M.A. Hussain, R. Nye, V. Mehta, K.T. Mamun and N. Hossain, *Cureus*, **9**, e1403 (2017); <https://doi.org/10.7759/cureus.1403>.
- F. Prestinaci, P. Pezzotti and A. Pantosti, *Pathog. Glob. Health*, **109**, 309 (2015); <https://doi.org/10.1179/2047773215Y.0000000030>.
- A. Franceschi, M. Tuccori, G. Bocci, F. Vannozzi, A. Di Paolo, C. Barbara, M. Lastella, C. Blandizzi and M. Del Tacca, *Pharmacol. Res.*, **49**, 85 (2004); <https://doi.org/10.1016/j.phrs.2003.08.001>.
- J.R. Anacona, K. Mago and J. Camus, *Appl. Organomet. Chem.*, **32**, e4374 (2018); <https://doi.org/10.1002/aoc.4374>.
- M.A. Malik, O.A. Dar, P. Gull, M.Y. Wani and A.A. Hashmi, *MedChemComm*, **9**, 409 (2018); <https://doi.org/10.1039/C7MD00526A>.
- A.N. Srivastva, N.P. Singh and C.K. Shrivastaw, *Arab. J. Chem.*, **9**, 48 (2016); <https://doi.org/10.1016/j.arabjc.2014.10.004>.
- R. Jin, J. Liu, G. Zhang, J. Li, S. Zhang and H. Guo, *Chem. Biodivers.*, **15**, e1800263 (2018); <https://doi.org/10.1002/cbdv.201800263>.
- R. Miyazaki, H. Yasui and Y. Yoshikawa, *Open J. Inorg. Chem.*, **6**, Article ID 65425 (2016); <https://doi.org/10.4236/ojic.2016.62007>.
- S. Murtaza, M.S. Akhtar, F. Kanwal, A. Abbas, S. Ashiq and S. Shamim, *J. Saudi Chem. Soc.*, **21**, S359 (2017); <https://doi.org/10.1016/j.jscs.2014.04.003>.
- N. Mohammed Hosny, Y.E. Sherif and A.A. El-Rahman, *J. Coord. Chem.*, **61**, 2536 (2008); <https://doi.org/10.1080/00958970801930047>.
- H. Luo, Y.F. Xia, B.F. Sun, L.R. Huang, X.H. Wang, H.Y. Lou, X.H. Zhu, W.D. Pan and X.D. Zhang, *Biochem. Res. Int.*, **2017**, 1 (2017); <https://doi.org/10.1155/2017/6257240>.
- A. Aouniti, H. Elmsellem, S. Tighadouini, M. Elazzouzi, S. Radi, A. Chetouani, B. Hammouti and A. Zarrouk, *J. Taibah Univ. Sci.*, **10**, 774 (2016); <https://doi.org/10.1016/j.jtusc.2015.11.008>.
- Y. Jia and J. Li, *Chem. Rev.*, **115**, 1597 (2015); <https://doi.org/10.1021/cr400559g>.
- E.A. Lane, M.J. Canty and S.J. More, *Res. Vet. Sci.*, **101**, 132 (2015); <https://doi.org/10.1016/j.rvsc.2015.06.004>.
- L. Izrael-Zivkovic, M. Rikalovic, G. Gojic-Cvijovic, S. Kazazic, M. Vrvic, I. Brèeski, V. Beskoski, B. Lonèarevic, K. Gopèevic and I. Karad•ic, *RSC Adv.*, **8**, 10549 (2018); <https://doi.org/10.1039/C8RA00371H>.
- S.G. Teoh, S.H. Ang, H.K. Fun and C.W. Ong, *J. Organomet. Chem.*, **580**, 17 (1999); [https://doi.org/10.1016/S0022-328X\(98\)01099-7](https://doi.org/10.1016/S0022-328X(98)01099-7).
- N.K. Chaudhary and P. Mishra, *J. Saudi Chem. Soc.*, **22**, 601 (2018); <https://doi.org/10.1016/j.jscs.2017.10.003>.
- N.K. Chaudhary and P. Mishra, *Bioinorg. Chem. Appl.*, **2017**, Article ID 6927675 (2017); <https://doi.org/10.1155/2017/6927675>.
- K. Dhahagani, S. Mathan Kumar, G. Chakkaravarthi, K. Anitha, J. Rajesh, A. Ramu and G. Rajagopal, *Spectrochim. Acta A Mol. Biomol. Spectrosc.*, **117**, 87 (2014); <https://doi.org/10.1016/j.saa.2013.07.101>.
- A.W. Bauer, W.M.M. Kirby, J.C. Sherris and M. Turck, *Am. J. Clin. Pathol.*, **45(4 ts)**, 493 (1966); [https://doi.org/10.1093/ajcp/45.4\\_ts.493](https://doi.org/10.1093/ajcp/45.4_ts.493).
- G.N. Rolinson and E.J. Russell, *Antimicrob. Agents Chemother.*, **2**, 51 (1972); <https://doi.org/10.1128/AAC.2.2.51>.
- G.G. Mohamed, M. Zayed and S.M. Abdallah, *J. Mol. Struct.*, **979**, 62 (2010); <https://doi.org/10.1016/j.molstruc.2010.06.002>.
- M.S. Nair, D. Arish and R.S. Joseyphus, *J. Saudi Chem. Soc.*, **16**, 83 (2012); <https://doi.org/10.1016/j.jscs.2010.11.002>.
- J.P. Coates, A Practical Approach to the Interpretation of Infrared Spectra, In: Encyclopedia of Analytical Chemistry. John Wiley & Sons Ltd.: Chichester, pp. 10815–10837 (2000).
- H.S. Seleem, *Chem. Cent. J.*, **5**, 35 (2011); <https://doi.org/10.1186/1752-153X-5-35>.
- F. Rahaman and B.H.M. Mruthyunjayaswamy, *Complex Met.*, **1**, 88 (2014); <https://doi.org/10.1080/2164232X.2014.889580>.
- L.A. Saghatforoush, A. Aminkhani, S. Ershad, G. Karimnezhad, S. Ghammamy and R. Kabiri, *Molecules*, **13**, 804 (2008); <https://doi.org/10.3390/molecules13040804>.
- C.M. Sharaby, *Biomol. Spectrosc.*, **66**, 1271 (2007); <https://doi.org/10.1016/j.saa.2006.05.030>.
- M. Sedighipoor, A.H. Kianfar, M.R. Sabzalian and F. Abyar, *Spectrochim. Acta A: Mol. Biomol. Spectrosc.*, **198**, 38 (2018); <https://doi.org/10.1016/j.saa.2018.02.050>.
- N.C. Ii, N. Ii, C. Ii, G. Ahumada, M. Fuentealba, T. Roisnel, S. Kahlal, D. Carrillo, R. Cordova, J. Saillard, J. Hamon and C. Manzur, *Polyhedron*, **151**, 279 (2018); <https://doi.org/10.1016/j.poly.2018.05.048>.
- R. Ebrahimi-Kahrizangi and M.H. Abbasi, *Trans. Nonferr. Met. Soc. China*, **18**, 217 (2008); [https://doi.org/10.1016/S1003-6326\(08\)60039-4](https://doi.org/10.1016/S1003-6326(08)60039-4).
- A. Coats and J.P. Redfern, *Analyst*, **88**, 906 (1963); <https://doi.org/10.1039/an9638800906>.
- M. Montazerzohori, S. Zahedi, A. Naghiha and M.M. Zohour, *Mater. Sci. Eng. C*, **35**, 195 (2014); <https://doi.org/10.1016/j.msec.2013.10.030>.
- P. Raj, A. Singh, A. Singh, N. Singh, *Sustain. Chem. Eng.*, (2017); <https://doi.org/10.1021/acssuschemeng.7b00963>.
- G. Sirikci, N.A. Ancin and S.G. Öztas, *J. Mol. Model.*, **21**, 221 (2015); <https://doi.org/10.1007/s00894-015-2764-4>.
- P. Mendu, J. Pragathi, B. Anupama and C.G. Kumari, *E-J. Chem.*, **9**, 2145 (2012); <https://doi.org/10.1155/2012/839789>.
- M. Padmaja, J. Pragathi, C.G. Kumari and A. Pradesh, *J. Chem. Pharm. Res.*, **3**, 602 (2011).
- S.S. Panda, O.S. Detistov, A.S. Girgis, P.P. Mohapatra, A. Samir and A.R. Katritzky, *Bioorg. Med. Chem. Lett.*, **26**, 2198 (2016); <https://doi.org/10.1016/j.bmcl.2016.03.062>.
- N. Fey, *J. Chem. Technol. Biotechnol.*, **74**, 852 (1999); [https://doi.org/10.1002/\(SICI\)1097-4660\(199909\)74:9<852::AID-JCTB131>3.0.CO;2-T](https://doi.org/10.1002/(SICI)1097-4660(199909)74:9<852::AID-JCTB131>3.0.CO;2-T).
- A.M. Majcher, P. Dabczyński, M.M. Marzec, M. Ceglarska, J. Rysz, A. Bernasik, S. Ohkoshi and O. Stefańczyk, *Chem. Sci.*, **9**, 7277 (2018); <https://doi.org/10.1039/C8SC02277A>.